npg

ORIGINAL ARTICLE

Temperature and light-induced self-assembly changes of a tetra-arm diblock copolymer in an ionic liquid

Xiaofeng Ma, Ryoji Usui, Yuzo Kitazawa, Hisashi Kokubo and Masayoshi Watanabe

A tetra-arm diblock copolymer ([PEG-*b*-P(AzoMA-*r*-NIPAm)]$_4$) was synthesized by reversible addition–fragmentation chain transfer copolymerization of *N*-isopropylacrylamide (NIPAm) and 4-phenylazophenyl methacrylate (AzoMA), initiating from the ends of functionalized tetra-arm polyethylene glycol (tetra-PEG). The resulting tetra-arm diblock copolymer consists of two segments: tetra-PEG (the center block; compatible with 1-butyl-3-methylimidazolium hexafluorophosphate ([C$_4$mim]PF$_6$)) and P(AzoMA-*r*-NIPAm) (the end blocks; temperature- and photosensitive compatibility with [C$_4$mim]PF$_6$ due to photoresponsive upper critical solution temperature phase behavior). We found that [PEG-*b*-P(AzoMA-*r*-NIPAm)]$_4$ underwent high-temperature unimer and low-temperature micelle (upper critical micellization temperature (UCMT)) transitions in [C$_4$mim]PF$_6$. The UCMT of the tetra-arm diblock copolymer depended on photoisomerization states of the azobenzene groups within the copolymer. The UCMT of the *trans*-form polymer in dark conditions was higher than that of the *cis*-form polymer under UV-light irradiation. We demonstrated photoinduced self-assembly changes of the tetra-arm diblock copolymer in [C$_4$mim]PF$_6$ at a 'bistable' temperature. Reversible photoinduced unimer/micelle transitions were also demonstrated.
Polymer Journal (2015) **47**, 739–746; doi:10.1038/pj.2015.55; published online 29 July 2015

INTRODUCTION

Ionic liquids (ILs) are ambient temperature molten salts and have attracted considerable attention because of their unique properties such as nonvolatility, nonflammability, thermal and chemical stability and high ionic conductivity.[1–8] Composite materials consisting of polymers and ILs can realize useful materials such as polymer electrolyte membranes, gas separation membranes and catalytic membranes.[9,10] Furthermore, we previously focused on stimuli-responsive polymers in ILs.[11,12] For example, poly(*N*-isopropylacrylamide) (PNIPAm) shows an upper critical solution temperature (UCST) phase transition in certain ILs, which is a completely opposite phenomenon to that observed in aqueous solutions.[13] In contrast, certain polymethacrylates[14–16] or polyether derivatives[17–19] are found to exhibit lower critical solution temperature (LCST) phase behavior in ILs. Phase transitions of polymers in nonvolatile and thermally stable ILs can afford long-term stable smart materials without solvent evaporation. Recently, we developed photoresponsive polymers in ILs by copolymerization of an azobenzene-containing monomer, 4-phenylazophenyl methacrylate (AzoMA), with either NIPAm[20] or benzyl methacrylate[21] as the main monomer.

Self-assembly of block copolymer in an IL is another fascinating topic from the materials science point of view.[22–26] Block copolymer membranes or dilute solutions exhibit useful nanostructures due to intramolecular segregation. Lodge and coworkers reported polybutadiene-*block*-poly(ethylene oxide) (PB-*b*-PEO) block copolymer self-assembly in 1-butyl-3-methylimidazolium hexafluorophosphate

([C$_4$mim]PF$_6$).[27] They found that PB-*b*-PEO self-assembled into micelles with an IL-insoluble PB core surrounded by PEO corona chains in [C$_4$mim]PF$_6$. Direct visualization using cryogenic transmission electron microscopy revealed various nano-ordered self-assembled structures with universal morphologies such as spheres, cylindrical micelles and bilayer vesicles in [C$_4$mim]PF$_6$. They also developed physical ion gels by gelation of an ABA triblock copolymer with an IL-selective B block and an IL-phobic A block in an IL. For example, polystyrene-*block*-poly(ethylene oxide)-*block*-polystyrene triblock copolymer dissolved in a PEO selective IL can form an ion gel through noncovalent association of the polystyrene blocks.[28] Physical ion gels comprising ABA triblock copolymers and ILs have numerous applications including organic transistors,[29] actuators[30] and low-voltage, flexible electrochemiluminescent device.[31] Certain thermosensitive block copolymers in ILs can realize thermoinduced micellization,[32] doubly thermosensitive micelles,[33,34] and thermoreversible ion gels.[35–37] We also reported that an azobenzene-containing diblock copolymer (PEO-*b*-P(AzoMA-*r*-NIPAm)) exhibits thermo- and photoinduced micellization in [C$_4$mim]PF$_6$.[38] Owing to the UCST phase behavior of random copolymer segments composed of AzoMA and NIPAm (P(AzoMA-*r*-NIPAm)), the diblock copolymer formed micelles at lower temperatures than the UCST of P(AzoMA-*r*-NIPAm). [C$_4$mim]PF$_6$ was selected because the UCST locates at experimentally suitable temperatures. Conversely, the block copolymer became unimers at higher temperatures than the UCST. The upper critical micellization temperature (UCMT) depended on the

Department of Chemistry and Biotechnology, Yokohama National University, Yokohama, Japan
Correspondence: Professor M Watanabe, Department of Chemistry and Biotechnology, Yokohama National University, 79-5 Tokiwadai Hodogaya-ku, Yokohama 240-8501, Japan.
E-mail: mwatanabe@ynu.ac.jp

photoisomerization states of azobenzene in the copolymer. The UCMT difference between the *trans*-form polymer and the *cis*-form polymer was 4 °C. At a suitable temperature, photoinduced reversible unimer/micelle transition was realized by illumination using light with appropriate wavelength. Very recently, we succeeded in realizing the sol–gel transition of concentrated ABA triblock copolymer solutions (20 wt%) in an IL triggered by a photostimulus.[39] The ABA triblock copolymer employed was P(AzoMA-*r*-NIPAm)-*b*-PEO-*b*-P(AzoMA-*r*-NIPAm), and the sol–gel transition was caused by the photoinduced aggregation state change of the ABA triblock copolymer. The photo processable ion gel is a very fascinating material; however, mechanical strength of the ion gel was not sufficient.[39]

How block copolymer architecture affects the aggregation states is of great interest. We need to accumulate such knowledge because the information on self-assembly of block copolymer in ILs is rather poor, compared with that in water and organic solvents. Furthermore, in order to utilize the photoinduced sol–gel transition for material processing, the enhancement of mechanical integrity of the gel state is our great concern. Herein, we describe thermo- and photoinduced self-assembly changes of a tetra-arm diblock copolymer ([PEG-*b*-P(AzoMA-*r*-NIPAm)]$_4$) in [C$_4$mim]PF$_6$. The [PEG-*b*-P(AzoMA-*r*-NIPAm)]$_4$ diblock copolymer, with tetra-polyethylene glycol (tetra-PEG) as the central block and P(AzoMA-*r*-NIPAm) as the four end blocks, was prepared by reversible addition–fragmentation chain transfer (RAFT) copolymerization of NIPAm and AzoMA, initiating from end functionalized tetra-PEG precursor. Our paper first describes the thermosensitive self-assembly of the tetra-arm diblock copolymer in [C$_4$mim]PF$_6$. Then it describes the reversible photoinduced unimer/micelle transitions by alternating irradiation by UV and visible light at a suitable temperature. Although micellization of tetra-arm diblock copolymers can be found in aqueous solutions,[40–47] self-assembly of tetra-arm diblock copolymers in ILs are yet to be reported.

EXPERIMENTAL PROCEDURE
Materials
Tetra-PEG (number-average molecular weight (M_n) = 40 000, average molecular weight of each arm = 10 000; polydispersity index (M_w/M_n) = 1.05) was provided by NOF Corporation (Tokyo, Japan) and dried by azeotropic distillation using toluene to remove residual water. NIPAm was provided by Kohjin Chemicals Corporation (Tokyo, Japan) and purified by recrystallization (two times) using a toluene/hexane (1:10 by weight) mixed solvent. 2,2′-Azobis (isobutyronitrile) was purchased from Sigma-Aldrich (Tokyo, Japan) and recrystallized from methanol. 1,4-Dioxane, dehydrated dichloromethane and oxalyl chloride were purchased from Wako Chemicals (Osaka, Japan) and used without further purification. S-1-dodecyl-S′-(α,α′-dimethyl-α″-acetic acid) trithiocarbonate (CTA) was synthesized according to a previously reported procedure.[48,49] AzoMA was synthesized by a reported procedure.[50,51] [C$_4$mim] PF$_6$ was prepared according to a previous report.[52] The water content of the [C$_4$mim]PF$_6$ was determined by a Karl Fischer titration and was < 10 p.p.m.

Synthesis of [PEG-*b*-P(AzoMA-*r*-NIPAm)]$_4$ tetra-arm diblock copolymer
The block copolymer was prepared according to the procedure shown in Scheme 1. The first step was to synthesize the tetra-PEG-CTA macroinitiator. Tetra-PEG (6.64 g, 0.166 mmol) and dry dichloromethane (50 ml) was placed into a two-necked flask and stirred at room temperature until a transparent solution was obtained. CTA (0.620 g, 1.70 mmol) was mixed with excess oxalyl chloride (0.44 ml, 5.1 mmol) in dry dichloromethane (10 ml) in another two-necked flask under an argon atmosphere and stirred at room temperature until gas evolution stopped (~2 h). Dichloromethane and excess oxalyl chloride were then removed under vacuum, and the residue was re-dissolved in dry dichloromethane (12 ml). This solution was then added to tetra-PEG solution. The reaction was allowed to stir for 24 h at room temperature, after which the

contents were reprecipitated three times by pouring the tetra-PEG-CTA solution in tetrahydrofuran (as a good solvent) into cold diethyl ether (as a poor solvent). The precipitate was then dried under vacuum at room temperature overnight to yield tetra-PEG-CTA as a light-yellow powder (6.33 g, 90%).

The second step was RAFT copolymerization of NIPAm and AzoMA from the end of the obtained tetra-PEG-CTA. Tetra-PEG-CTA (1.00 g, 0.0242 mmol), AzoMA (1.36 g, 5.11 mmol) and NIPAm (15.9 g, 0.141 mol) ([AzoMA]/[NIPAm] = 3.5/96.5) were dissolved in 1,4-dioxane (100 ml) in a round-bottom flask and bubbled with argon for 30 min at 45 °C. Special attention was given to avoid crystallization of the NIPAm monomer during the bubbling process. 2,2′-Azobis(isobutyronitrile) (5.0 mg, 0.030 mmol) and 1,4-dioxane (5.0 ml) was separately placed in a separate round-bottom flask and bubbled with argon for 30 min at room temperature. The 2,2′-Azobis (isobutyronitrile) solution (3.3 ml, 0.020 mmol) was then added to the monomer solution. RAFT polymerization was carried out at 65 °C for 68 h. The reaction mixture was evaporated and purified by reprecipitation three times from acetone (as a good solvent) to cold diethyl ether (as a poor solvent). Then, the collected yellow powder was purified by fractional precipitation. The precipitate was dissolved in ethanol with 5 wt% concentration at 40 °C. After the solution was stored in a refrigerator about 2 days, the solid precipitate was observed. Then the upper solution was decanted and the precipitate was collected. The precipitate was purified again by reprecipitation with acetone and cold diethyl ether. The precipitate was then dried overnight under vacuum at 40 °C to yield [PEG-*b*-P(AzoMA-*r*-NIPAm)-CTA]$_4$ as a yellow powder (2.10 g, 11%).

Finally, the removal of the RAFT agent at each chain end of the polymer ([PEG-*b*-P(AzoMA-*r*-NIPAm)-CTA]$_4$) was conducted according to the following procedure. [PEG-*b*-P(AzoMA-*r*-NIPAm)-CTA]$_4$ (1.00 g, 0.0107 mmol), 2,2′-Azobis(isobutyronitrile) (0.212 g, 1.29 mmol) and 1,4-dioxane (25 ml) were mixed in a round-bottom flask and bubbled with argon for 30 min at room temperature. The reaction was allowed to proceed under argon atmosphere at 80 °C for 12 h. The reaction mixture was evaporated and purified by reprecipitation three times from acetone (as a good solvent) to cold diethyl ether (as a poor solvent). The precipitate was then dried overnight under vacuum at 40 °C to yield [PEG-*b*-P(AzoMA-*r*-NIPAm)]$_4$ as a yellow powder (0.870 g, 87%).

Sample preparation
A solution of [PEG-*b*-P(AzoMA-*r*-NIPAm)]$_4$ in [C$_4$mim]PF$_6$ was prepared using the co-solvent method. The tetra-arm diblock copolymer was first dissolved in tetrahydrofuran, followed by the addition of an appropriate amount of [C$_4$mim]PF$_6$ (polymer/IL = 1/99 by weight). The solution was then stirred continuously for at least 3 h until a transparent solution was obtained. The volatile tetrahydrofuran was then removed by evaporation at 80 °C under vacuum for 24 h. Sample solution was filtered by using 0.20-µm filter to eliminate dust before dynamic light scattering (DLS) measurements.

Measurements
The synthesized polymers were characterized by ^{1}H NMR and gel permeation chromatography (GPC). ^{1}H NMR (500 MHz) spectrum was recorded with a Bruker DXR 500 (Karlsruhe, Germany). The M_w/M_n of the synthesized polymers was determined by GPC using a Shimadzu HPLC system (columns: Tosoh calibrated by polystyrene standards (Kyoto, Japan)). The system was operated at a flow rate of 1.0 ml min^{-1} using dimethylformamide containing 0.01 mol l^{-1} LiBr as the eluent.

DLS was performed using an Otsuka Electronics DLS-6500 (Osaka, Japan) equipped with an ALV-6010/160 correlator (Langen, Germany) and a He–Ne laser with wavelength of 633 nm. Temperatures were controlled to within an accuracy of ± 0.1 °C using an index-matching silicon oil bath. Experiments were performed at various temperatures from 75 to 50 °C in a cooling process. The intensity correlation functions $g_2(q,t)$ were recorded at a scattering angle of 90° at each temperature for 30 s to obtain the relationship between R_h values and temperatures. The intensity correlation function data for photoreversible micellization were collected every 30 s to make the time resolution of each measurement, which is faster than that of the photoinduced micellization
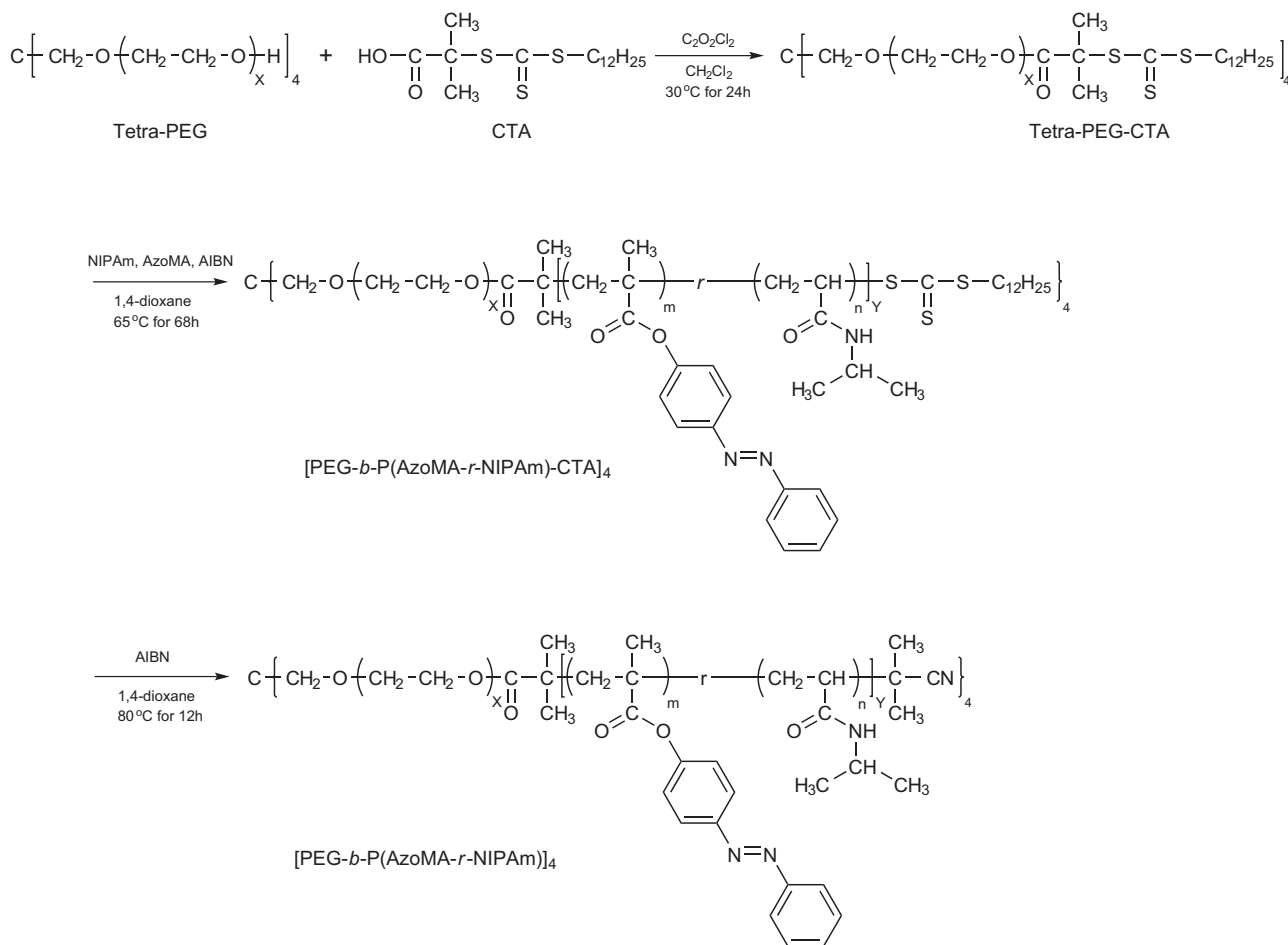
Scheme 1 Synthetic procedure for the tetra-arm diblock copolymer.

process. Data was collected after equilibrating at each temperature for at least 30 min.

For solutions containing monodisperse particles, the electric field correlation function $g_1(q, t)$ exhibits a single exponential decay,

$$g_1(q, t) = \exp(-\Gamma t) = \exp(-D_0 q^2 t) \qquad (1)$$

where t is the time, q is the scattering vector ($q = (4\pi n/\lambda)\sin(\theta/2)$; n is the refractive index of the solutions, λ is the wavelength of the light in vacuum and θ is the scattering angle), Γ is the decay rate and D_0 is the mutual diffusion coefficient at infinite dilution. The recorded intensity correlation function $g_2(q, t)$ was converted to $g_1(q, t)$ through the Siegert relation.[53] The hydrodynamic radius, R_h, can be estimated using the solvent viscosity, η and the Stokes–Einstein equation,

$$R_h = (k_b T)/6\pi\eta D_0 \qquad (2)$$

where k_b and T are the Boltzmann constant and absolute temperature, respectively. For solutions with polydisperse (not monomodal) particles, $g_1(q, t)$ can be analyzed by the method of cumulants,[54]

$$g_1(q, t) = A \exp(-\Gamma t)\left(1 + (1/2!)\mu_2 t^2 - (1/3!)\mu_3 t^3\right), \qquad (3)$$

where Γ is the mean decay rate and μ_2/Γ^2 represents the width of the distribution. In this work, the apparent hydrodynamic radius, R_h, was determined using equation (2) by replacing D_0 with $D = \Gamma/q^2$ of the 1 wt% solutions. The distribution of R_h was also obtained by applying the inverse Laplace transformation to $g_1(q, t)$ with the well-established CONTIN program,[55] and by a sum of two exponentials. To estimate R_h, the temperature dependence of the viscosity of [C$_4$mim]PF$_6$ was calculated using the appropriate Vogel–Tammann–Fulcher equation,[52]

$$\eta = 0.36 \exp[639/(T - 201)] \qquad (4)$$

where T (K) is the absolute temperature. The refractive index of [C$_4$mim]PF$_6$ was calculated using equation,[56]

$$n = 1.49569 - 3.2 \times 10^{-4} T + 8.8 \times 10^{-8} T^2 \qquad (5)$$

where T (K) is the absolute temperature. Photoirradiation was carried out using a 500 W high-pressure mercury lamp (Ushio Optical Modulex BA-H500). The wavelength and intensity of the irradiated light (UV-light: 366 nm, 8 mW cm^{-2}; visible light: 437 nm, 4 mW cm^{-2}) were adjusted using color filters. Either UV (366 nm) or visible light (437 nm) was irradiated from the upper side of the DLS sample tube (1 cm diameter). A transparent heat-absorbing filter covered the top of the sample tube to avoid the generation of heat from the mercury lamp and contamination by dust.

RESULTS AND DISCUSSION

Characterization of the tetra-arm diblock copolymer

The products of each reaction step in Scheme 1 were identified by ^{1}H NMR (Supplementary Figures S-1, and Figure 1). The end group conversion ratio of tetra-PEG-CTA was calculated from the ^{1}H NMR spectrum (Supplementary Figure S-1) by comparing integrated signal intensities of the ethylene protons in the tetra-PEG main chain (e) with that of the methyl protons in CTA (a) and was found to be unity. Changes in the GPC traces with each reaction step are shown in Figure 2, and an ^{1}H NMR spectrum of the target block copolymer
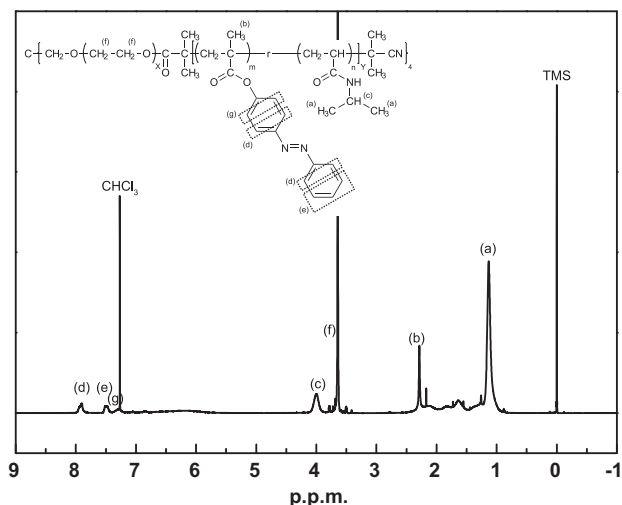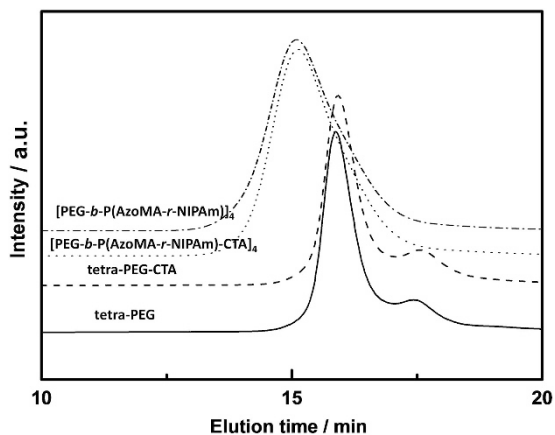
Figure 1 ¹H NMR spectrum of [PEG-*b*-P(AzoMA-*r*-NIPAm)]₄ in CDCl₃.

Figure 2 GPC traces of tetra-PEG (solid line), tetra-PEG-CTA (dashed line), [PEG-*b*-P(AzoMA-*r*-NIPAm)-CTA]₄ (dotted line) and [PEG-*b*-P(AzoMA-*r*-NIPAm)]₄ (dashed and dotted line).

([PEG-*b*-P(AzoMA-*b*-NIPAm)]₄) is shown in Figure 1. The M_n of [PEG-*b*-P(AzoMA-*b*-NIPAm)]₄ was calculated from the ¹H NMR spectrum (Figure 1) by comparing the integrated signal intensities of the tetra-PEG main chain ((f) 3.6 p.p.m.) with that of the end blocks ((c) 4.0 p.p.m. from NIPAm; (d) 7.9 p.p.m. from AzoMA). The AzoMA composition was calculated from the ratio of integrated signal intensities between NIPAm and AzoMA, which showed that 8.7 mol% of AzoMA was incorporated into the random copolymer. The characterized results of the original tetra-PEG and the synthesized tetra-arm polymers are summarized in Table 1.

In the GPC trace of tetra-PEG, a satellite peak was observed at a longer elution time than that of the main peak, which corresponded to PEG having $M_n = 10$ kDa, one-fourth of M_n of tetra-PEG, which appeared to be originated from trace amount of water in the preparation system. This satellite peak still persisted in the GPC trace of tetra-PEG-CTA. In contrast, the GPC traces of [PEG-*b*-P(AzoMA-*r*-NIPAm)-CTA]₄ and [PEG-*b*-P(AzoMA-*r*-NIPAm)]₄ were unimodal, indicating that low molecular weight block copolymers starting from the low molecular weight PEG were effectively removed by the fractional precipitation (Supplementary Figure S-3). Although

Table 1 Molecular characterization of tetra-PEG and tetra-arm block copolymer ([PEG-*b*-P(AzoMA-*r*-NIPAm)]₄)

Polymer	M_n (kDa)	M_w/M_n[a]	[AzoMA]/[NIPAm][b]
Tetra-PEG	40.0	1.05	—
[PEG-*b*-P(AzoMA-*r*-NIPAm)]₄	92.0[b]	1.41	8.7/91.3

Abbreviations: AzoMA, 4-phenylazophenyl methacrylate; DMF, dimethylformamide; GPC, gel permeation chromatography; NIPAm, *N*-isopropylacrylamide; PEG, polyethylene glycol; PSt, polystyrene.
[a]Determined by GPC (calibrated with PSt standards and eluent: DMF containing 0.01 mol l⁻¹ LiBr).
[b]Determined by ¹HNMR.

polymers prepared by living radical polymerization usually have a lower M_w/M_n than 1.2. However, [PEG-*b*-P(AzoMA-*r*-NIPAm)]₄ has $M_w/M_n = 1.4$. This is due to the fact that the polymerization is less controlled due to retarding or inhibiting effect of the azobenzene group for radicals.[57] All of the data supported reasonable preparation of the tetra-arm diblock copolymer ([PEG-*b*-P(AzoMA-*r*-NIPAm)]₄).

Thermosensitivity of the tetra-arm diblock copolymer in [C₄mim]PF₆

DLS was employed to investigate micellization of tetra-arm diblock copolymer in [C₄mim]PF₆. Figure 3 shows the normalized scattering intensity and hydrodynamic radius of a 1 wt% tetra-arm diblock copolymer solution in [C₄mim]PF₆ with or without UV-light irradiation at a scattering angle of 90°. The normalized scattering intensities were defined as the intensity at each temperature divided by that at 75 °C. Under dark conditions, the isomerization state of the azobenzene was composed of the *trans*-state (100%), whereas under UV-light irradiation the *cis*-state (80%) dominated.[21,58] In the cooling process from 75 °C, the scattered intensity increased with decrease of sample temperature in the dark and under UV-light irradiation (Figure 3a), thanks to the UCST phase behavior of the P(AzoMA-*r*-NIPAm) segments. This indicates that the tetra-arm diblock copolymer aggregates into large size micelles, which scatter the incident light. The aggregation behavior was thermally reversible. The mean hydrodynamic radius (R_h) of the *trans*- and *cis*-form polymer were also determined (Figure 3b). At higher temperatures than the UCMT, the distribution function was bimodal both in the dark and under UV-light irradiation (Figures 4 and 5). The smaller R_h peak corresponds to the single polymer chains (unimers), whereas the larger R_h peak indicates the existence of aggregates. (dashed lines in Figure 3b) However, the weight fraction of the unimers is calculated to be over 0.999 using a previously reported method,[59] and it was considered that almost all of the scattering in [C₄mim]PF₆ above the UCMT came from single polymer chains. There are two possible reasons for this small amount of aggregates at higher temperatures. One reason is that these aggregates might arise from solubility differences because of chain-to-chain variations in the comonomer distribution and composition in the random copolymer block; the other reason is these aggregates may result from the tiny fraction of polymers with very high molecular weight that are reluctant to dissolve. The R_h of the unimer in the [C₄mim]PF₆ is < 10 nm, consistent with the size of [PEG-*b*-P(AzoMA-*r*-NIPAm)]₄ single polymer chains with a molecular weight of 92 kDa.

When the temperature was lower than the UCMT, only an intense peak around the R_h of large particles remained and the smaller R_h peak was completely disappeared. This indicates that unimers aggregated into micelles. The R_h of the micelle at lower temperatures are approximately 35 nm, possibly suggesting spherical core–shell micelles
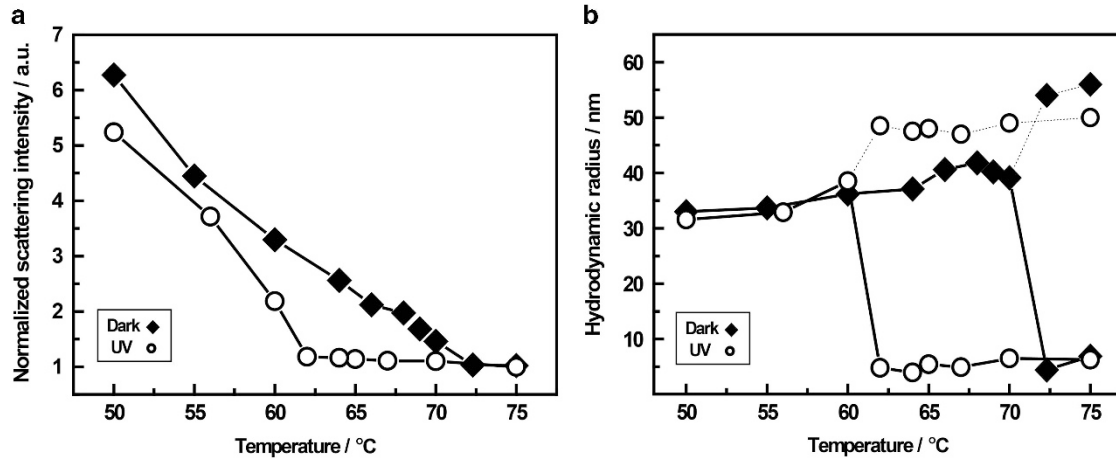
Figure 3 (**a**) Temperature dependence of normalized scattering intensity for [PEG-*b*-P(AzoMA-*r*-NIPAm)]$_4$ (1 wt%) in [C$_4$mim]PF$_6$ under dark conditions (solid diamonds) and with UV-light irradiation (open circles) at a scattering angle of 90° in the cooling process. (**b**) Temperature dependence of the hydrodynamic radius (R_h) for [PEG-*b*-P(AzoMA-*r*-NIPAm)]$_4$ (1 wt%) in [C$_4$mim]PF$_6$ under dark conditions (solid diamonds) and with UV-light irradiation (open circles). Dotted line indicates minor components in the system.
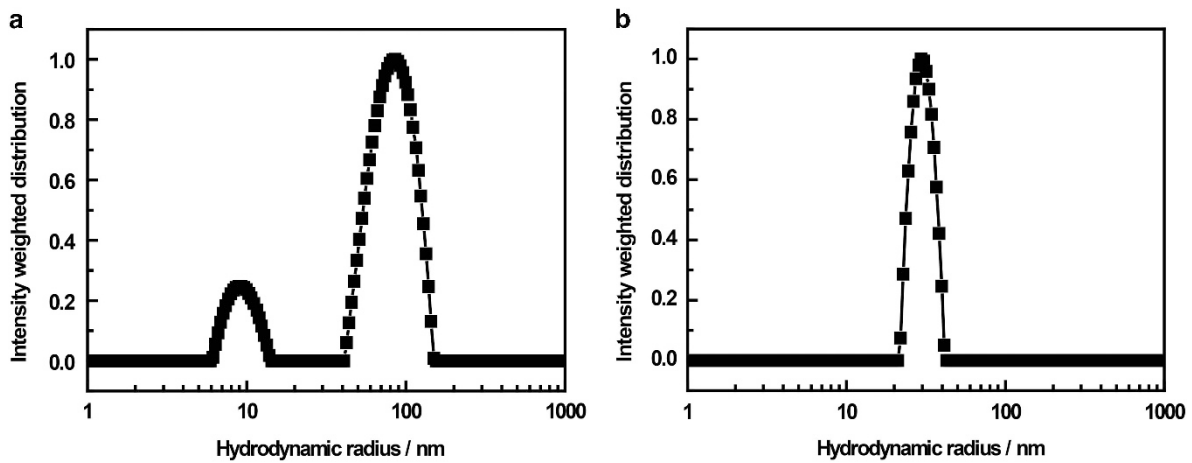

Figure 4 CONTIN results for [PEG-*b*-P(AzoMA-*r*-NIPAm)]$_4$ in [C$_4$mim]PF$_6$ (1 wt%) solution at (**a**) 75 °C and (**b**) 50 °C under dark conditions.
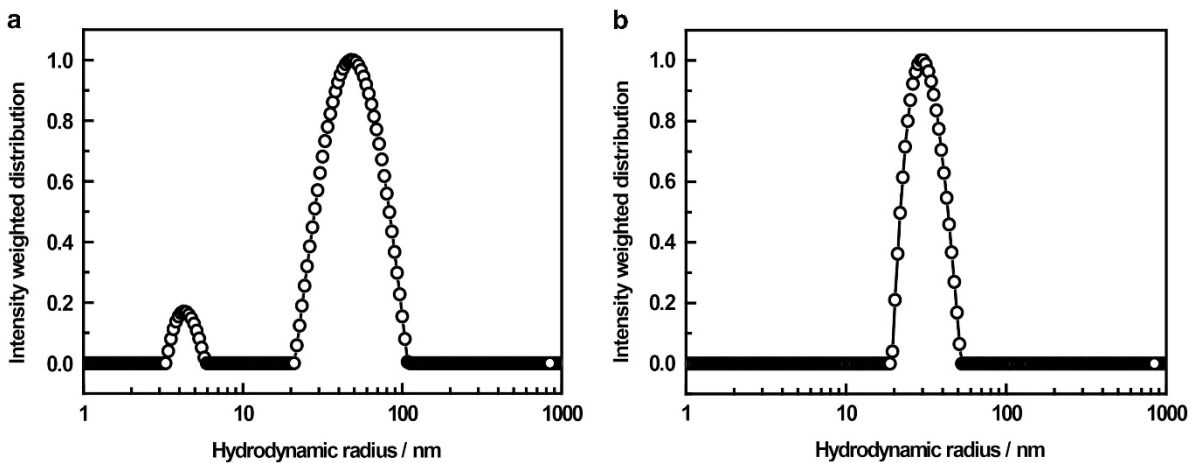

Figure 5 CONTIN results for [PEG-*b*-P(AzoMA-*r*-NIPAm)]$_4$ in [C$_4$mim]PF$_6$ (1 wt%) solution at (**a**) 75 °C and (**b**) 50 °C under UV-light irradiation.

with solvatophobic P(AzoMA-*r*-NIPAm) core. The core could be surrounded by solvatophilic tetra-PEG segments that are not free end-arm shells, as they have a tetra-arm nodule in the center of the block copolymer. We have previously reported thermo/photoinduced micellization of an azobenzene-containing diblock copolymer (PEO-*b*-P(AzoMA-*r*-NIPAm), total $M_n = 35$ kDa, PEO weight fraction = 0.43) in [C$_4$mim]PF$_6$.[38] In that report, below the UCMT, PEO-*b*-P(AzoMA-*r*-NIPAm) diblock copolymers self-assembled into micelles having $R_h = 120$ nm, which could have vesicular morphology judged from the M_n.[38] Since the present tetra-arm block copolymer has the same PEO weight fraction of 0.43 as that of the diblock copolymer, the difference in the R_h values could mainly be attributed to a difference in the block copolymer architecture (simple diblock copolymer and tetra-arm diblock copolymer). The PEO segments in the diblock copolymer have free chain ends, whereas those in the tetra-arm block copolymer do not. Such difference appears to cause the difference in the micellar structures. After passing through the UCMT, the scattering intensity monotonically increases (Figure 3a); nevertheless, the R_h of the tetra-arm diblock copolymer is almost kept constant with decreasing temperature (Figure 3b). Since the scattering intensity is generally proportional to the sixth power of the size of the micelle and linear to the number of particles. Thus, this result may suggest that the number of particles gradually increases with keeping the size of micelle constant during the cooling process.[59]

The UCMTs of the tetra-arm diblock copolymer were 70 and 60 °C for the *trans*- and *cis*-form polymer in [C$_4$mim]PF$_6$, respectively (Figure 3b). Importantly, there is a 10 °C difference between the UCMT of the *trans*-form polymer and that of the *cis*-form polymer (bistable temperature range). The UCMT difference arises from the difference in polarity of photoisomerization states of AzoMA. It is well-known that the polarity of azobenzene depends on its photo-isomerization state; the dipole moment of the planar *trans*- azobenzene (0.5 D) is markedly smaller than that of *cis*- azobenzene (3.1 D). This could result in the higher polarity of the latter and its improved solubility in ILs. [C$_4$mim]PF$_6$ has dipole moment (μ) of 5.3 D and dielectric constant (ε) of 11.4, indicating moderate polarity.[60,61] Therefore, the *trans*-form polymers have higher UCMT in ILs than the *cis*-form polymers. In our previous report, the UCMT difference of the diblock copolymer with or without UV irradiation was as small as 4 °C.[38] The different temperature ranges between both systems can be attributed to the difference in azobenzene composition of the block copolymers. The azobenzene composition in the stimuli-responsive segment for the previously reported diblock copolymer was 2.0 mol%, whereas that in the present tetra-arm diblock copolymer was 8.7 mol %. These results are consistent with the previous report on the UCST phase transition of a P(AzoMA-*r*-NIPAm) random copolymer, where the cloud point difference between the *trans*- and *cis*-form polymers changed from 4 to 24 °C with a change in the AzoMA composition (from 1.9 to 8.6 mol%).[38] By using this transition temperature difference, we further confirmed the reversibility of photoinduced unimer/micelle transition.

Unimer-micelle transition of [PEG-*b*-P(AzoMA-*r*-NIPAm)]$_4$ in [C$_4$mim]PF$_6$ induced by photo-stimuli

Figure 6 shows a reversible unimer-micelle transition induced by light stimuli at a bistable temperature. First, the polymer solution was kept at a bistable temperature (64 °C) under UV-light irradiation; the R_h of the tetra-arm diblock copolymer was < 10 nm. The size distribution always displays a bimodal distribution (Figure 7a). This is consistent with distribution function of Figure 5a. The weight fraction of single polymer chains could also be estimated to be over 0.999, which indicates that aggregation is negligible. At time 0 s, the solution was irradiated by visible light to form the *trans*-polymer. The size of micelles formed by photoinduced transition was ~ 35 nm. This was quite similar to the size of the micelles generated under the thermal induced transition of [PEG-*b*-P(*trans*-AzoMA-*r*-NIPAm)]$_4$, as shown in Figure 4b. The size distribution function exhibits a unimodal distribution (Figure 7b), which indicates formation of micelles. There is an induction time (500 s) before aggregation of the tetra-arm diblock copolymer. We previously reported that photoinduced unimer-micelle transition of PEO-*b*-P(AzoMA-*r*-NIPAm) diblock copolymer in an IL required two elementary steps.[38] The first step was the photoisomerization of azobenzene from *cis* to *trans*, while the second step was diffusion of polymers to self-assemble into micelles.[38] We considered these two steps, because the photoisomerization of the *cis*- to the *trans*-form of the azobenzene-containing random copolymer in the IL reached a photostationary state within 240 s under UV-light irradiation,[20,21] using the same experimental set-up and conditions as the present study. Therefore, polymer diffusion step is the rate-determining step for photoinduced micellization.

After the induction time, the scattering intensity monotonically increased until 2300 s, whilst the average R_h abruptly increased
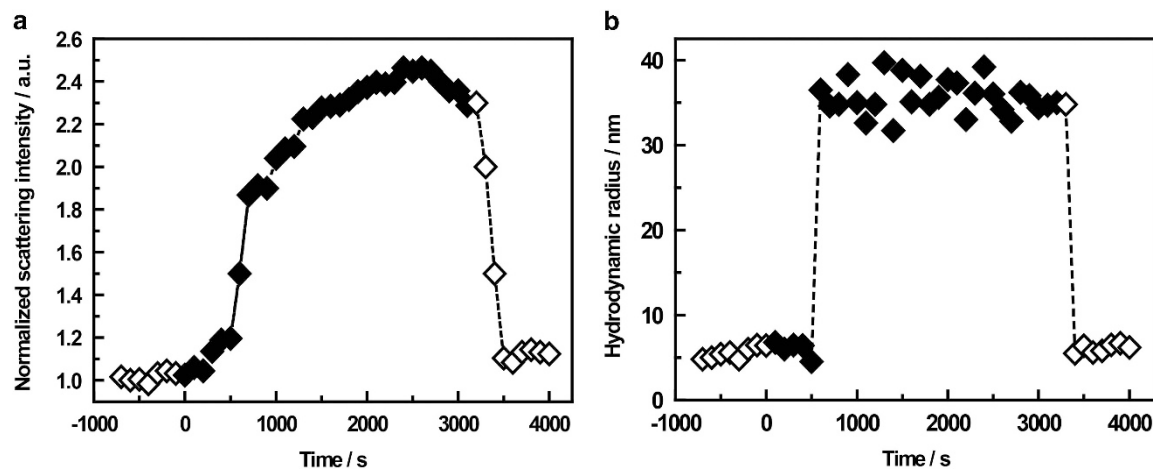

Figure 6 Reversible photoinduced self-assembly and dissociation of [PEG-*b*-P(AzoMA-*r*-NIPAm)]$_4$ polymer micelles at 64 °C under UV (open diamonds) or visible light (solid diamonds) irradiation; (**a**) normalized scattering intensity and (**b**) mean R_h, as a function of time.
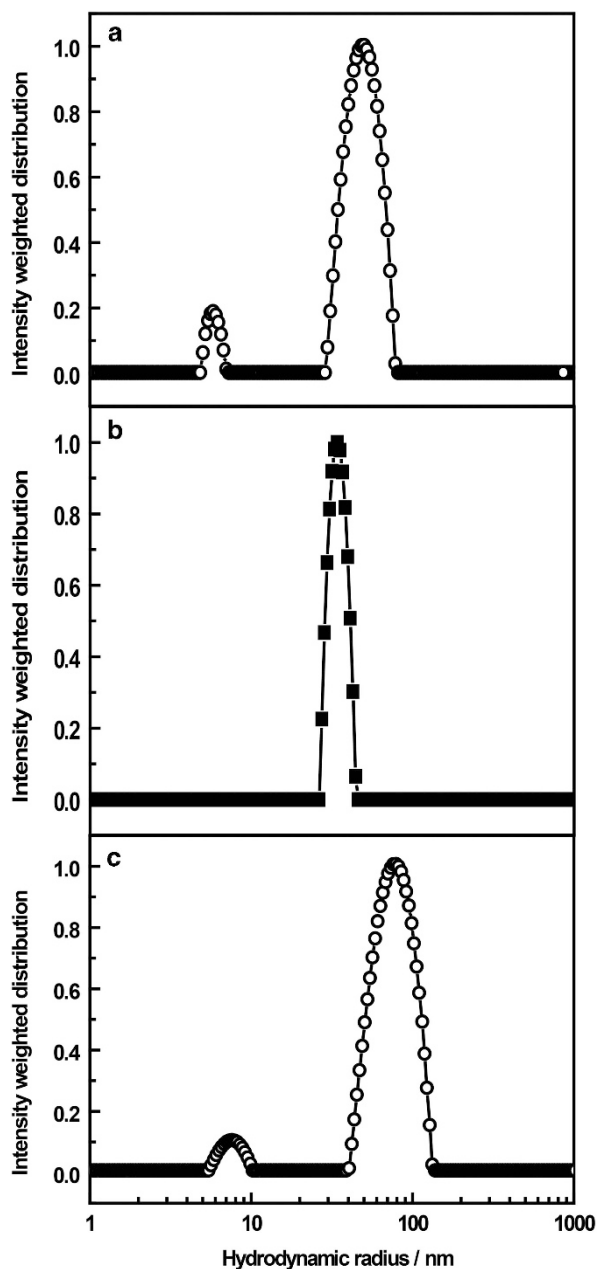
polymer chains, because the UCMT of the *cis*-form polymer was lower than 64 °C (measurement temperature). The distribution function also confirmed this transition (Figure 7c). This phenomenon demonstrated that the photoinduced unimer/micelle transition was reversible. The demicellization process was much faster than the micellization process, because no polymer diffusion step was required.

CONCLUSION

A tetra-arm diblock copolymer ([PEG-*b*-P(AzoMA-*r*-NIPAm)]$_4$) was successfully prepared by RAFT polymerization. The tetra-arm diblock copolymer had tetra-PEG as the solvatophilic central block and P (AzoMA-*r*-NIPAm) as four temperature- and photoresponsive end blocks. We studied its self-assembly in [C$_4$mim]PF$_6$ under diluted conditions. It was shown that the UCMT of the *trans*-form polymer was 10 °C higher than that of *cis*-form polymer from the DLS measurements. Finally, a photoinduced reversible unimer/micelle transition of the tetra-arm diblock copolymer utilizing the UCMT difference between the *trans*- and the *cis*-form polymer in an IL was demonstrated. A study on the development of photoreversible sol–gel transition using self-assembly of the tetra-arm diblock copolymers for concentrated solutions is now in progress.

CONFLICT OF INTEREST

The authors declare no competing financial interest.

Figure 7 CONTIN results for [PEG-*b*-P(AzoMA-*r*-NIPAm)]$_4$ in a [C$_4$mim]PF$_6$ (1 wt%) solution at 64 °C: (**a**) under UV-light irradiation (before visible light irradiation); (**b**) under visible light irradiation; and (**c**) after switching back to UV-light irradiation again.

(Figure 6). Early in the aggregation process, system includes a large amount of unimers and few large aggregates. The scattering intensity strongly depends on the size of particles rather than the number of particles. Therefore, once the unimers aggregation starts, the DLS signal is heavily weighted by the larger particles.[59] Thus, the increase of scattering intensity from 500 to 2300 s is roughly proportional to the increase of the number of micelles. The completion of aggregation process seems to be reached after about 2300 s.

After the micelles were formed under visible light irradiation, we switched back to UV-light irradiation at 3250 s to form the *cis*-form polymer. Both the scattering intensity and the R_h decreased (Figure 6). This indicated that the disassociation of micelles into individual single

1 Welton, T. Room-temperature ionic liquids. solvents for synthesis and catalysis. *Chem. Rev.* **99**, 2071–2083 (1999).
2 Holbrey, J. D. & Seddon, K. R. Ionic liquids. *Clean Products Process* **1**, 223–236 (1999).
3 Seddon, K. R. Ionic liquids: a taste of the future. *Nat. Mater.* **2**, 363–365 (2003).
4 Wasserscheid, P. & Keim, W. Ionic liquids - new "solutions" for transition metal catalysis. *Angew. Chem. Int. Ed. Engl.* **39**, 3772–3789 (2000).
5 Magee, J. W., Kabo, G. J. & Frenkel, M. in *ACS Symposium Series 901: Ionic liquids IIIA: Fundamentals, Progress, Challenges, and Opportunities Properties and Structure* (eds Rogers R. D. & Seddon K. R.) Ch. 12, 160–174 (American Chemical Society, Washington, DC, USA, 2005).
6 Dietz, M. L., Dzielawa, J. A., Jensen, M. P., Beitz, J. V. & Borkowski, M. in *ACS Symposium Series 902: Ionic liquids IIIB: Fundamentals, Progress, Challenges, and Opportunities Transformations and Processed* (eds Rogers R. D. & Seddon K. R.) Ch. 1, 2–18 (American Chemical Society, Washington, DC, USA, 2005).
7 Wilkes, J. S. A short history of ionic liquids-from molten salts to neoteric solvents. *Green Chem.* **4**, 73–80 (2002).
8 Plechkova, N. V. & Seddon, K. R. Applications of ionic liquids in the chemical industry. *Chem. Soc. Rev.* **37**, 123–150 (2008).
9 Holbrey, J. D., Chen, J., Turner, M. B., Swatloski, R. P., Spear, S. K. & Rogers, R. D. in *ACS Symposium Series 913: Ionic liquids in Polymer Systems: Solvents, Additives, and Novel Application* (eds Brazel C. S. & Rogers R. D.) Ch. 5, 71–87 (American Chemical Society, Washington, DC, USA, 2005).
10 Winterton, N. Solubilization of polymers by ionic liquids. *J. Mater. Chem.* **16**, 4281–4293 (2006).
11 Lodge, T. P. Materials science: a unique platform for materials design. *Science* **321**, 50–51 (2008).
12 Ueki, T. & Watanabe, M. Polymers in ionic liquids: dawn of neoteric solvents and innovative materials. *Bull. Chem. Soc. Jpn.* **85**, 33–50 (2012).
13 Ueki, T. & Watanabe, M. Upper critical solution temperature behavior of poly(N-isopropylacrylamide) in an ionic liquid and preparation of thermo-sensitive nonvolatile gels. *Chem. Lett.* **35**, 964–965 (2006).
14 Ueki, T. & Watanabe, M. Lower critical solution temperature behavior of linear polymers in ionic liquids and the corresponding volume phase transition of polymer gels. *Langmuir* **23**, 988–990 (2007).

15 Kodama, K., Nanashima, H., Ueki, T., Kokubo, H. & Watanabe, M. Lower critical solution temperature phase behavior of linear polymers in imidazolium-based ionic liquids: effects of structural modifications. *Langmuir* **25**, 3820–3824 (2009).

16 Lee, H. -N. & Lodge, T. P. Poly(*n*-butyl methacrylate) in ionic liquids with tunable lower critical solution temperatures (LCST). *J. Phys. Chem. B* **115**, 1971–1977 (2011).

17 Kodama, K., Tsuda, R., Niitsuma, K., Tamura, T., Ueki, T., Kokubo, H. & Watanabe, M. Structural effects of polyethers and ionic liquids in their binary mixtures on lower critical solution temperature liquid-liquid phase separation. *Polym. J.* **43**, 242–248 (2011).

18 Lee, H.-N., Newell, N., Bai, Z. & Lodge, T. P. Unusual lower critical solution temperature phase behavior of poly(ethylene oxide) in ionic liquids. *Macromolecules* **45**, 3627–3633 (2012).

19 Rodriguez, H. & Rogers, R. D. Liquid mixtures of ionic liquids and polymers as solvent systems. *Fluid Phase Equilibria* **294**, 7–14 (2010).

20 Ueki, T., Nakamura, Y., Yamaguchi, A., Niitsuma, K., Lodge, T. P. & Watanabe, M. UCST phase transition of azobenzene-containing random copolymer in an ionic liquid. *Macromolecules* **44**, 6908–6914 (2011).

21 Ueki, T., Yamaguchi, A., Ito, N., Kodama, K., Sakamoto, J., Ueno, K., Kokubo, H. & Watanabe, M. Photoisomerization-induced tunable LCST phase separation of azobenzene-containing polymers in an ionic liquid. *Langmuir* **25**, 8845–8848 (2009).

22 Riess, G. Micellization of block copolymers. *Prog. Polym. Sci.* **28**, 1107–1170 (2003).

23 Hamley, I. W. *Block Copolymers in Solutions: Fundamentals and Applications*, (John Wiley & Sons, Chichester, UK, 2005).

24 Alexandridis, P. & Lindman, B. in *Amphiphilic Block Copolymers: Self-Assembly and Applications* (eds Alexandridis, P. & Lindman, B.) Ch. 1, 1–12 (Elsevier, Amsterdam, The Netherlands, 2000).

25 Zhang, L. & Eisenberg, A. Multiple morphologies of "crew-cut" aggregates of polystyrene-*b*-poly(acrylic acid) block copolymers. *Science* **268**, 1728–1731 (1995).

26 Bates, F. S. Polymer-polymer phase behavior. *Science* **251**, 898–905 (1991).

27 He, Y., Li, Z., Simone, P. & Lodge, T. P. Self-assembly of block copolymer micelles in an ionic liquid. *J. Am. Chem. Soc.* **128**, 2745–2750 (2006).

28 He, Y., Boswell, P. G., Buhlmann, P. & Lodge, T. P. Ion gels by self-assembly of a triblock copolymer in an ionic liquid. *J. Phys. Chem. B* **111**, 4645–4652 (2007).

29 Cho, J. -H., Lee, J., Xia, Y., Kim, B. -S., He, Y., Renn, M. J., Lodge, T. P. & Frisbie, C. D. Printable ion-gel gate dielectrics for low-voltage polymer thin-film transistors on plastic. *Nat. Mater.* **7**, 900–906 (2008).

30 Imaizumi, S., Kokubo, H. & Watanabe, M. Polymer actuators using ion-gel electrolytes prepared by self-assembly of ABA-triblock copolymers. *Macromolecules* **45**, 401–409 (2012).

31 Moon, H. C., Lodge, T. P. & Frisbie C. D. Solution-processable electrochemiluminescent ion gels for flexible, low-voltage, emissive displays on plastic. *J. Am. Chem. Soc.* **136**, 3705–3712 (2014).

32 Tamura, S., Ueki, T., Ueno, K., Kodama, K. & Watanabe, M. Thermosensitive self-assembly of diblock copolymers with lower critical micellization temperatures in ionic liquid. *Macromolecules* **42**, 6239–6244 (2009).

33 Ueki, T., Watanabe, M. & Lodge, T. P. Doubly thermosensitive self-assembly of diblock copolymers in ionic liquids. *Macromolecules* **42**, 1315–1320 (2009).

34 Lee, H. -N., Bai, Z., Newell, N. & Lodge, T. P. Micelle/inverse micelle self-assembly of a PEO-PNIPAm block copolymer in ionic liquids with double thermoresponsivity. *Macromolecules* **43**, 9522–9528 (2010).

35 He, Y. & Lodge, T. P. A thermoreversible ion gel by triblock copolymer self-assembly in an ionic liquid. *Chem. Commun.* **43**, 2732–2734 (2007).

36 He, Y. & Lodge, T. P. Thermoreversible ion gels with tunable melting temperatures from triblock and pentablock copolymers. *Macromolecules* **41**, 167–174 (2008).

37 Kitazawa, Y., Ueki, T., Niitsuma, K., Imaizumi, S., Lodge, T. P. & Watanabe, M. Thermoreversible high-temperature gelation of an ionic liquid with poly(benzyl methacrylate-*b*-methyl methacrylate-*b*-benzyl methacrylate) triblock copolymer. *Soft Matter* **8**, 8067–8074 (2012).

38 Ueki, T., Nakamura, Y., Lodge, T. P. & Watanabe, M. Light-controlled reversible micellization of a diblock copolymer in an ionic liquid. *Macromolecules* **45**, 7566–7573 (2012).

39 Ueki, T., Nakamura, Y., Usui, R., Kitazawa, Y., So, S., Lodge, T. P. & Watanabe, M. Photoreversible gelation of a triblock copolymer in an ionic liquid. *Angew. Chem. Int. Ed. Engl.* **54**, 3018–3022 (2015).

40 Strandman, S., Zarembo, A., Darinskii, A. A., Loflund, B., Butcher, S. J. & Tenhu, H. Self-assembling of star-like amphiphilic block copolymers with polyelectrolyte blocks. Effect of pH. *Polymer* **48**, 7008–7016 (2007).

41 He, E., Ravi, P. & Tam, K. C. Synthesis and self-assembly behavior of four-arm poly (ethylene oxide)-*b*-poly(2-(diethylamino)ethyl methacrylate) star block copolymer in salt solutions. *Langmuir* **23**, 2382–2388 (2007).

42 Mori, H., Ebina, Y., Kambara, R. & Nakabayashi, K. Temperature-responsive self-assembly of star block copolymers with poly(ionic liquid) segments. *Polymer J* **44**, 550–560 (2012).

43 Jeong, Y., Nah, J., Lee, H., Kim, S. & Cho, C. Adriamycin release from flower-type polymeric micelle based on star-block copolymer composed of poly(*γ*-benzyl *L*-glutamate) as the hydrophobic part and poly(ethylene oxide) as the hydrophilic part. *Int. J. Pharm.* **188**, 49–58 (1999).

44 He, E., Yue, C. Y. & Tam, K. C. Association behavior of star-shaped ph-responsive block copolymer: four-arm poly(ethylene oxide)-*b*-poly(methacrylic acid) in aqueous medium. *Langmuir* **25**, 4892–4899 (2009).

45 Deng, M., Chen, X., Piao, L., Zhang, X., Dai, Z. & Jing, X. Synthesis of four-armed poly (*ε*-caprolactone)-*block*-poly(ethylene oxide) by diethylzinc catalyst. *J. Polym. Sci. A Polym. Chem* **4**, 950–959 (2004).

46 Kim, K., Cui, G., Lim, H., Huh, J., Ahn, C. H. & Jo, W. Synthesis and micellization of star-shaped poly(ethylene glycol)-*block*-poly(*ε*-caprolactone). *Macromol. Chem. Phys.* **205**, 1684–1692 (2004).

47 Jones, M. C., Ranger, M. & Leroux, J. C. pH-Sensitive unimolecular polymeric micelles: synthesis of a novel drug carrier. *Bioconjug. Chem.* **14**, 774–781 (2003).

48 Ryayev, J. & Hillmyer, M. A. Nanochannel array plastics with tailored surface chemistry. *J. Am. Chem. Soc.* **127**, 13373–13379 (2005).

49 Lai, J. T., Filla, D. & Shea, R. Functional polymers from novel carboxyl-terminated trithiocarbonates as highly efficient RAFT agents. *Macromolecules* **35**, 6754–6756 (2002).

50 Yuan, W., Jiang, G., Wang, J., Wang, G., Song, Y. & Jiang, L. Temperature/light dual-responsive surface with tunable wettability created by modification with an azobenzene-containing copolymer. *Macromolecules* **39**, 1300–1303 (2006).

51 Shimoboji, T., Ding, Z., Stayton, P. & Hoffman, A. Photoswitching of ligand association with a photoresponsive polymer-protein conjugate. *Bioconjug. Chem.* **13**, 915–919 (2002).

52 Tokuda, H., Hayamizu, K., Ishii, K., Susan, M. A. & Watanabe, M. Physicochemical properties and structures of room temperature ionic liquids. 1. Variation of anionic species. *J. Phys. Chem. B* **108**, 16593–16600 (2004).

53 Brown, W. *Dynamic Light Scattering: The Method and Some Applications*, (Clarendon Press, Oxford, UK, 1993)

54 Koppel, D. E. Analysis of macromolecular polydispersity in intensity correlation spectroscopy. Method of cumulants. *J. Chem. Phys.* **57**, 4814–4820 (1972).

55 Provencher, S. W. A constrained regularization method for inverting data represented by linear algebraic or integral equations. *Comput. Phys. Commun.* **27**, 213–227 (1982).

56 Pereiro, A. B., Legido, J. L. & Rodríguez, A. Physical properties of ionic liquids based on 1-alkyl-3-methylimidazolium cation and hexafluorophosphate as anion and temperature dependence. *J. Chem. Thermodynamics* **39**, 1168–1175 (2007).

57 Luo, C., Zuo, F., Ding, X., Zheng, Z., Cheng, X. & Peng, Y. Light-triggered reversible solubility of *α*-cyclodextrin and azobenzene moiety complexes in PDMAA-*co*-PAPA via molecular recognition. *J. Appl. Polym. Sci.* **4**, 2118–2125 (2008).

58 Ueki, T., Yamaguchi, A. & Watanabe, M. Unlocking of interlocked heteropolymer gel by light: photoinduced volume phase transition in an ionic liquid from a metastable state to an equilibrium phase. *Chem. Commun.* **48**, 5133–5135 (2012).

59 Shibayama, M., Karino, T. & Okabe, S. Distribution analyses of multi-modal dynamic light scattering data. *Polymer* **47**, 6446–6456 (2006).

60 Hunger, J., Stoppa, A., Schrodle, S., Hefter, G. & Buchner, R. Temperature dependence of the dielectric properties and dynamics of ionic liquids. *ChemPhysChem* **10**, 723–733 (2009).

61 Wakai, C., Oleinikikova, A., Ott, M. & Weingartner, H. How polar are ionic liquids? determination of the static dielectric constant of an imidazolium-based ionic liquid by microwave dielectric spectroscopy. *J. Phys. Chem. B* **109**, 17028–17030 (2005).

Supplementary Information accompanies the paper on Polymer Journal website (http://www.nature.com/pj)